Physics – Uspekhi **60** (12) 1277 – 1293 (2017)

INSTRUMENTS AND METHODS OF INVESTIGATION PACS numbers: 07.05.Fb, 07.05.Hd, 07.05.Kf, **29.40. – n**

Muon radiography method for fundamental and applied research

A B Alexandrov, M S Vladymyrov, V I Galkin, L A Goncharova, V M Grachev, S G Vasina, N S Konovalova, A A Malovichko, A K Managadze, N M Okat'eva, N G Polukhina, T M Roganova, N I Starkov, V E Tioukov, M M Chernyavsky, T V Shchedrina

DOI: https://doi.org/10.3367/UFNe.2017.07.038188

Contents

Abstract. This paper focuses on the basic principles of the muon radiography method, reviews the major muon radiography experiments, and presents the first results in Russia obtained by the authors using this method based on emulsion track detectors.

A B Alexandrov, M S Vladymyrov, L A Goncharova, S G Vasina, N S Konovalova, N M Okat'eva, N I Starkov, M M Chernyavsky, T V Shchedrina Lebedev Physical Institute, Russian Academy of Sciences, Leninskii prosp. 53, 119991 Moscow, Russian Federation
V I Galkin Skobeltsyn Institute of Nuclear Physics, Lomonosov Moscow State University, Leninskie gory 1, str. 2, 119991 Moscow, Russian Federation; Lomonosov Moscow State University, Faculty of Physics, Leninskie gory 1, str. 2, 119991 Moscow, Russian Federation
V M Grachev National Research Nuclear University MEPhI, Kashirskoe shosse 31, 115409 Moscow, Russian Federation
A A Malovichko Federal Research Center 'Geophysical Survey', Russian Academy of Sciences, prosp. Lenina 189, 249035 Obninsk, Kaluga region, Russian Federation
A K Managadze, T M Roganova Skobeltsyn Institute of Nuclear Physics, Lomonosov Moscow State University, Leninskie gory 1, str. 2, 119991 Moscow, Russian Federation
N G Polukhina Lebedev Physical Institute, Russian Academy of Sciences, Leninskii prosp. 53, 119991 Moscow, Russian Federation; National Research Nuclear University MEPhI, Kashirskoe shosse 31, 115409 Moscow, Russian Federation; National University of Science and Technology MISIS, Leninskii prosp. 4, 119049 Moscow, Russian Federation
E-mail: poluhina@sci.lebedev.ru
V E Tioukov Lebedev Physical Institute, Russian Academy of Sciences, Leninskii prosp. 53, 119991 Moscow, Russian Federation; Instituto Nazionale di Fisica Nucleare (INFN), Sezione di Naples, Università degli Studi di Napoli Federico II, Complesso Universitario di Monte Sant'Angelo, Via Cinthia, 21, Edificio 6, 80126 Napoli, Italy

Received 21 March 2017, revised 27 July 2017
Uspekhi Fizicheskikh Nauk **187** (12) 1375 – 1392 (2017)
DOI: https://doi.org/10.3367/UFNr.2017.07.038188
Translated by G Pontecorvo; edited by A Radzig

Keywords: muon radiography, nuclear photoemulsion, image recognition, track detectors

1. Introduction

Cosmic rays, which traditionally serve as a source of information concerning processes in outer space, also provide the possibility of studying physical processes occurring on Earth. Studies of the flux of muons of cosmic origin gave rise to the method of muon radiography (MR) — a method of nondestructive inspection based on 'raying' an object with ionizing muon radiation and registration of the radiation transmitted through the object. Analysis of the features of cosmic muon fluxes passing through matter permits the investigation of the internal state of large natural and industrial objects on the surface and within the depths of the Earth, which are of interest from the points of view of science and of applications, or are the source of potential danger for the surrounding infrastructure. When the inverse mathematical problem is successfully resolved, the method of muon radiography provides the capability to obtain three-dimensional images of the objects studied.

On the surface of the Earth, there are a large number of problematic geological and industrial zones, the state of which presents a serious threat to the environment and the social infrastructure, requiring continuous monitoring. The method proposed permits us to find regions of enhanced or reduced density within the bulk of the object examined by comparing the levels of absorption of cosmic muons by its different parts. The method can be applied for monitoring both the large natural objects, such as volcanoes and geological plates, and for the nondestructive inspection of industrial objects: wells and mines, installations of nuclear power facilities, industrial and architectural sites (tunnels, embankments, blast-furnaces, bridge supports, and so on), for monitoring fire-hazardous dumps containing carbonic rock, for analyzing seismic processes, and as a prospective

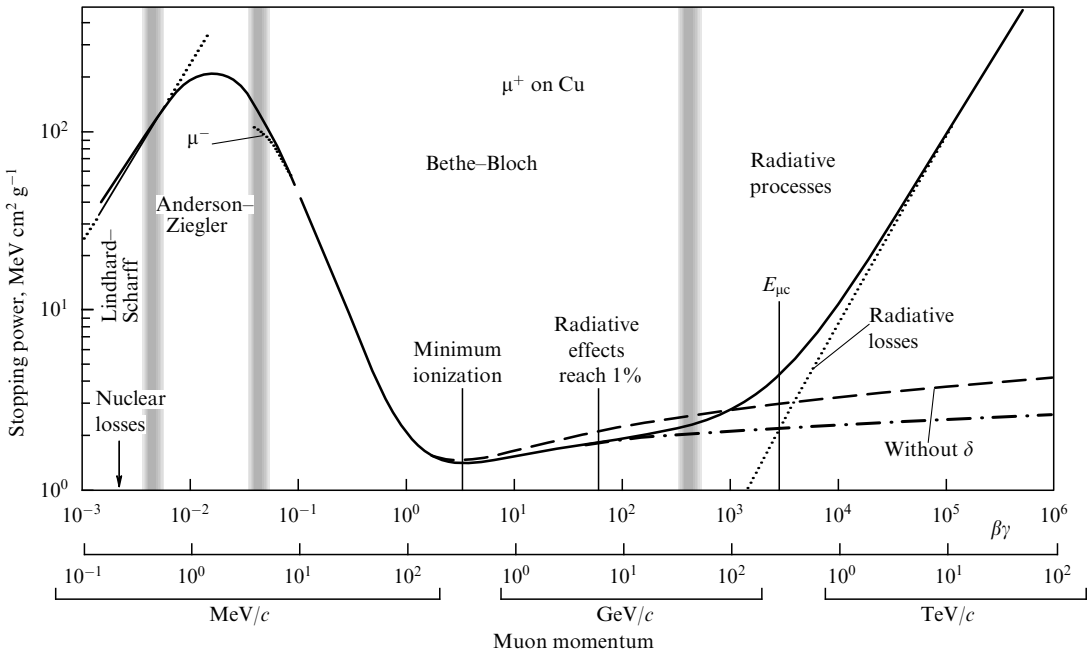

Figure 1. Muon energy losses in a copper absorber, comprising electronic (ionization and excitation) and radiative losses. The latter are due to e^+e^- pair production, bremsstrahlung, and photonuclear effects [4]. $\beta = v_\mu/c$, $\gamma = (1-\beta^2)^{-1/2}$. The vertical grey straight lines indicate the regions where the Lindhard–Scharff, Anderson–Ziegler, and Bethe–Bloch theories apply, as well as the region of radiative processes. Nuclear losses (nonionization losses of recoil nuclei) in the Lindhard–Scharff region are insignificant. The short dotted line, indicated as μ^-, illustrates the so-called Barkas effect [5, 6]. $E_{\mu c}$ is the critical muon energy, above which radiative losses start to be dominant; δ is a correction related to the influence of density on the electronic energy losses (ionization + excitation).

complement to geophysical methods in prospecting minerals. Traditional seismological methods, methods for temperature surveying, and electromagnetic and gravimetric probing are indirect and, unlike the MR method, involve significant uncertainties due to the superposition of signals pointing in different directions.

Thus, the MR method combines a uniquely high resolution (especially in the case of measurements with the use of nuclear photoemulsions), significantly superior to that of ordinary geophysical methods, the possibility of obtaining a detailed tomogram of the object being examined, and the application of the most novel methods for analyzing images. Applying the MR method in the monitoring mode may serve to prevent extreme situations or, at least, minimize their consequences for the population, infrastructure, and the environment.

The authors of the present article have for the first time in Russia developed techniques to resolve problems related to applying the MR method based on emulsion track detectors. The test experiments that were carried out have confirmed the efficiency of the method and the possibility of its application, making use of emulsion track detectors of the proposed construction and of means for processing emulsion data that are available in Russian institutions.

2. Justification of the method of muon radiography from the standpoint of physics

The MR method is based on the utilization of muon fluxes of cosmic origin, muons representing the main component of cosmic radiation at sea level (various data points to muons comprising from 63% [1] to 80% [2] of all the particles observed). Muons originate in the decays of charged π- and K-mesons that are produced in the atmosphere in interactions between nuclear-active particles from the primary cosmic radiation and the nuclei of atoms in Earth's atmosphere [3].

The actual lifetime of a muon is $\tau = 2.197 \times 10^{-6}$ s, i.e., the muon makes up an unstable particle. However, as the velocities of muons are close to the speed of light, these particles, owing to the relativistic slowing down of time, cover quite significant distances before they decay. The decay path of a muon with energy $\geqslant 1$ GeV is comparable to the thickness of the residual atmosphere from the level where the muons are generated down to the Earth's surface, which on the average varies from 10 to 20 km, and it increases with the muon energy.

Muons are not nuclear-active particles, and they lose energy in electromagnetic interactions, mainly by bremsstrahlung and through the ionization of atoms. The ionization losses of muons depend on their energy, but in the case of relativistic particles with energies up to ~ 100 GeV these losses can be considered a constant magnitude (on the order of 2 MeV cm^2 g^{-1}). For muons of such energies, ionization constitutes the dominant mechanism of energy losses, while in the case of high-energy muons (with energies $E_\mu \gtrsim 3$ TeV) energy losses due to ionization can be ignored, since in this case the determining contributions to energy losses are due to bremsstrahlung and pair production [4] (Fig. 1). Energy losses by bremsstrahlung are known to be inversely proportional to the mass squared of the particle. Since the rest mass of a muon is approximately 200 times greater than the rest mass of an electron ($m_\mu/m_e \approx 206.768$), a muon slowing-down in the field of a nucleus radiates approximately 4.3×10^4 times less energy than an electron in the same field. The fact that energy losses of muons due to bremsstrahlung are relatively small results in the ranges of muons in matter being significantly larger than the relevant ranges of electrons.

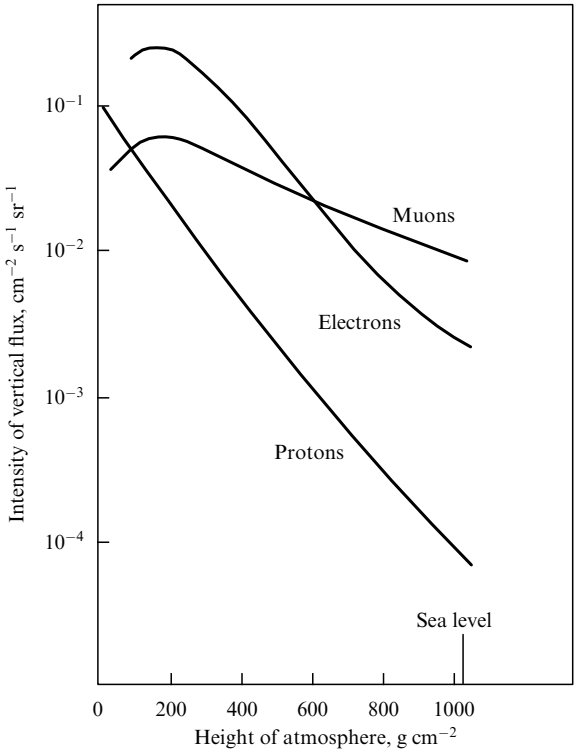

Figure 2. Intensity of the vertical muon flux at various heights in the atmosphere compared to the intensities of electron and proton fluxes [7].

These factors — the absence of strong interactions, the large rest mass, and velocity close to the speed of light — provide the high penetrating power of muons compared to that of hadrons, electrons, and γ-quanta (Fig. 2).

The penetrating power of the muon component of cosmic radiation depends on its energy spectrum on Earth's surface, and the penetration depth of each individual particle is proportional to its energy within a broad range of particle energies. Even at a relatively moderate energy $E \sim 10$ GeV, a muon can not only pass through the whole atmosphere, but also penetrate into the ground. Muons of cosmic origin with energies $E_\mu \sim 1-10$ TeV are registered in underground experiments at significant depths; thus, for example, muons were detected in the Kolar Gold Fields gold mine (India) at a depth exceeding 2300 m [8], and in the experiment MACRO (Monopole Astrophysics and Cosmic Ray Observatory) at a depth of more than 2500 m [9]. Figure 3 plots the minimum energies of muons on Earth's surface required for their penetration down to a given depth expressed in the units of meter water equivalent[1] [10]. The large range covered by muons before being absorbed in the rock environment, which is comparable to or even exceeds the dimensions of the objects examined, renders them a unique agent for radiography: since the spectrum of cosmic muons extends up to more than several hundred TeV, even in the case of such extended objects as mountain masses the muons capable of passing through them exist.

The dependence of the muon flux on the zenith angle is known to be described by $\cos^n\theta$, where the exponent n is close to 2. Thus, if the angle of incidence to the normal

[1] The depth expressed in the meter water equivalent (m w.e.) equals the product of the actual observation depth and the average density of the overlying rock.

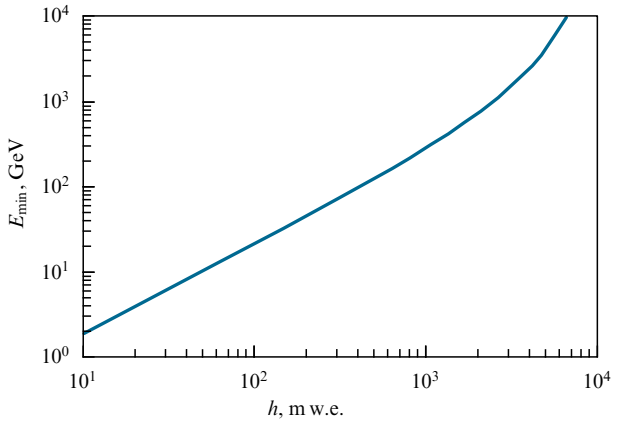

Figure 3. Minimum values of muon energy on Earth's surface necessary for reaching underground depth h [10].

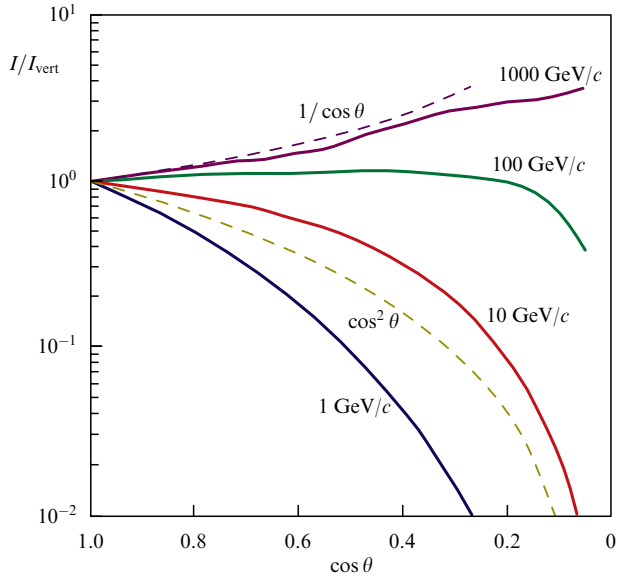

Figure 4. Ratio of muon flux intensity and vertical flux intensity at Earth's surface versus the cosine of zenith angle θ of a muon trajectory [10]. The angular distributions were estimated for muons with momenta 1, 10, 100, and 1000 GeV/c with the aid of the Monte Carlo method taking into account the curvature of Earth's atmosphere.

exceeds 60°, the muon component on Earth's surface is only one quarter as big, while the intensity of the nuclear component is reduced by a factor of 10^3. The intensity of the vertical flux of muons with energies $E_\mu > 1$ GeV amounts to about one particle per cm^2 per minute (I_{vert} for $E_\mu > 1$ GeV is on the order of 70 m^{-2} s^{-1} sr^{-1}) [9]. For higher muon energies ($E_\mu \gg 100$ GeV), the intensity of a nearly horizontal flux (at an angle $\theta \sim 80°$ to the vertical) significantly exceeds the intensity of the vertical flux (Fig. 4), which makes studies of the flux of nearly horizontal high-energy muons quite effective. In this case, as can be seen from Fig. 5, the absolute intensity of the muon flux decreases as the zenith angle increases and reaches a maximum at energies of 1–10 GeV. The intensity of muon fluxes determines the exposure time of the detectors, required for obtaining the most informative tomogram of the object.

The physics of MR is based on two effects: (1) the attenuation of muon fluxes in a thick absorber owing to electromagnetic processes (ionization, bremsstrahlung, elec-

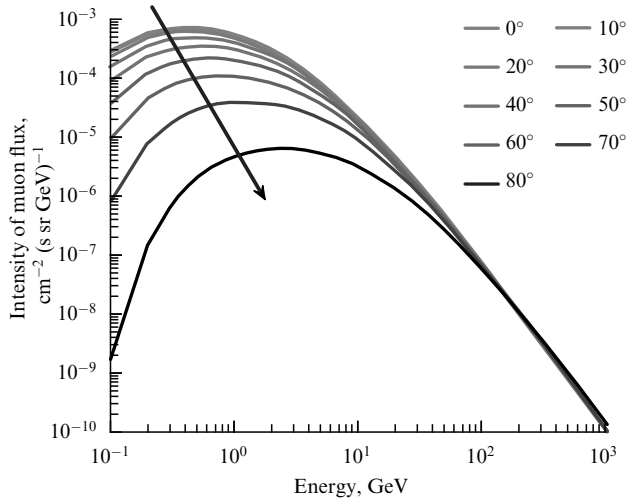

Figure 5. Intensity of muon fluxes in Earth's atmosphere versus muon energy for values of the zenith angle θ within the range from 0 to 80°. (Taken from Ref. [12].)

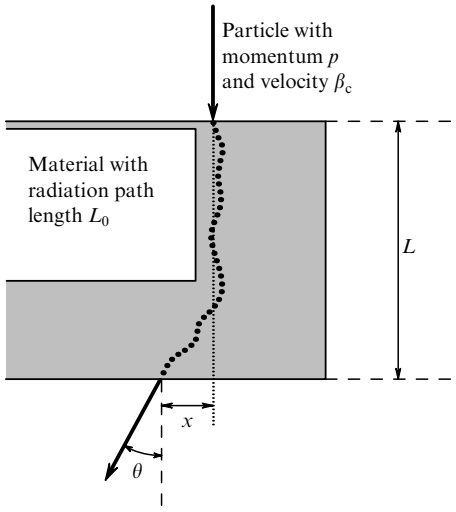

Figure 6. Result of multiple Coulomb scattering of a charged particle traversing a layer of material. (Taken from Ref. [16].)

tron–positron pair production), and (2) the differences among the characteristics of charged particle elastic scattering on the nuclei of different substances. The first effect consists in the flux of high-energy muons gradually weakening as they penetrate through the material because of energy losses due to electromagnetic processes, and the higher the charge number of the particles penetrating the material, the more significant the weakening of the flux of probing radiation. Calculating the vertical muon flux absorption as a function of the increasing mass of material above the registering equipment can be based on the muon energy spectrum. The differential muon energy spectrum at sea level, which has been well studied, can be described approximately by the following formula [13]:

$$\frac{\mathrm{d}N_\mu}{\mathrm{d}E_\mu\,\mathrm{d}\Omega} \approx \frac{0.14E_\mu^{-2.7}}{\mathrm{GeV\ cm^2\ s\ sr}}\left(\frac{1}{1+1.1E_\mu\cos\theta/(115\ \mathrm{GeV})} + \frac{0.054}{1+1.1E_\mu\cos\theta/(850\ \mathrm{GeV})}\right), \quad (1)$$

where N_μ is the number of muons, Ω is the solid angle, and the two terms in parentheses on the right-hand side represent contributions from the pions and charged kaons, respectively. Here, small contributions due to charm and heavier flavors are not taken into account, since they may be significant only at very high energies [14].

It should be noted that in performing experiments in muon radiography an accurate description of the spectrum of atmospheric muons may not be so important, if measurements are taken at sites before and after the object investigated.

If a material of a different density is encountered in the path of the cosmic muon flux, the intensity of electromagnetic interaction of the particles changes, which results in a change in the flux absorption intensity in this region. As is shown in Ref. [15], the vertical muon flux intensity $J_{\mathrm{vert}}(h)$ at relatively small depths ($h < 200$ m w.e.) follows a power law with a weakly varying exponent, and its dependence on the composition of the rock is relatively insignificant. For large depths ($h > 2000$ m w.e.), the intensity falls exponentially and substantially depends on the rock composition. In the intermediate range of depths, owing to the large contribution of losses proportional to the energy and to the rapid fall of the vertical spectrum at sea level at high energies, a qualitative change takes place in the shape of the dependence $J_{\mathrm{vert}}(h)$ — the power law is replaced by an exponential dependence.

The second effect is concerned with the fact that a charged particle moving in a medium undergoes a large number of elastic scatterings in the Coulomb fields of nuclei, resulting in its motion changing direction practically without any loss of energy (multiple Coulomb scattering) (Fig. 6).

Deviation of the muon trajectory from the initial direction can be described by a dependence close to a Gaussian one with a root-mean-square angular deviation [17]:

$$\langle\theta\rangle = \frac{14.1\ \mathrm{MeV}}{p\beta}\sqrt{\frac{L}{L_0}}\,, \quad (2)$$

where p is the muon momentum ($\approx 3-4$ GeV/c on Earth's surface [18]); β is the muon velocity (≈ 1); L is the thickness of an absorber, and L_0 is the radiation length unit for a given material. When the nuclear charge of the absorber increases, the degree of scattering (scattering per unit length) rises. However, numerous studies of muon scattering on the nuclei of different materials [19] have revealed the quantity $\langle\theta\rangle$ to be quite small even in the case of nuclei with a large charge Z ($\sim 1.5°$ for $Z > 82$). Therefore, the certain blurring of the image of a large object will not be very significant.

More precise simulations of the muon passage through matter are performed, in particular, with the aid of the well-known GEANT4 subpackages,[2] which were developed to simulate the passage of elementary particles and nuclei through complex installations in experiments at accelerators [20–22]. The authors of the present article use the GEANT4 package to simulate the passage of muons through layers of ground and iron [23]. Figure 7 shows the sum over φ of the distributions over θ of the numbers of muons with an initial energy $E = 98$ GeV that passed through layers of ground of thicknesses $L = 110$, 130, and 150 m (the total range of muons in the ground at this energy amounts to 172 m). This angular distribution can be approximated by the function

[2] GEANT stands for GEometry ANd Tracking.

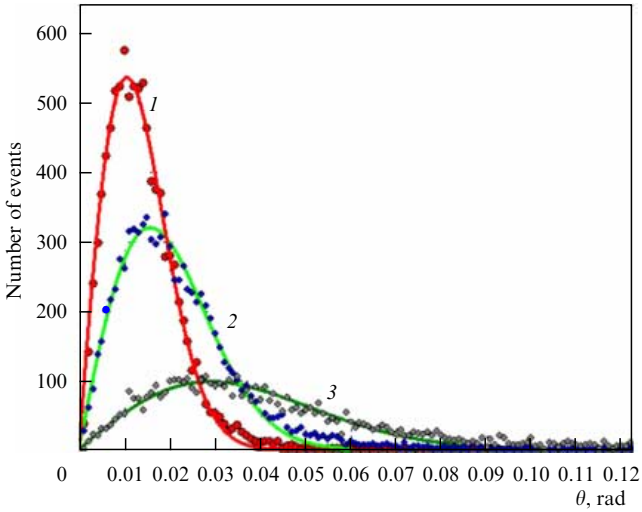

Figure 7. Distributions of the number of particles over the angle θ for muons covering distances of 110 m (curve *1*), 130 m (curve *2*), and 150 m (curve *3*) in passing through rocky ground. Approximation is performed by the function $F = A\theta \exp\left[-(\delta\theta)^2\right]$ [23].

$F = A\theta \exp\left[-(\delta\theta)^2\right]$. Such a form of the distribution of the number of particles corresponds to the flux distribution (i.e., the number of particles per unit area) in the form of a Gaussian function with the same parameter δ. The dependence of the parameter $\delta(E, L)$ on E for a fixed thickness L can be approximated by a linear function [23].

The flux intensity registered by the detector in a certain direction permits judging the degree of muon absorption and, consequently, the character of the ground and of extraneous inclusions present in this direction. A comparison of the density of the muon flux Φ after its traversing a target with the flux Φ_0 falling freely from the atmosphere in the same direction permits determining the average density of the object in the given direction. The flux of muons departing from the object under investigation is formed by particles, the energy of which is sufficient to traverse the object. The final number of muons registered in the direction toward the object depends on the muon flux incoming the target, the exposure time, the path length of muons within the object, and the density of the material of the detector and its sensitivity.

Unlike tomography in medicine [24], in which the source of radiation used has given characteristics, the proposed technique of muon radiography is based on radiation that is spread out in energy and the angle of incidence, which requires information on the angular distribution of the probe radiation.

There are two essentially different methods of transmitting objects:

(a) the absorption method [25], in which the differential absorption of particles in the object is measured. This method underlies muon radiography and medical radiography (utilizing X-rays). It is impossible with the aid of this method to extract information carried by an individual particle, so one can only obtain an average picture — a two-dimensional differential map of densities — and to reconstruct it one must know the input spectrum. This map is angular in the case of muon radiography, and coordinate in the case of medical radiography;

(b) the scattering method, in which two detectors are exploited: one above the object, and the other underneath, tuned to coincidences, and for each individual particle measurements are performed of its coordinate and/or its incidence angles both at the entrance point to the object and at the exit point. This method is not so sensitive to the density as to Z, and it immediately provides three-dimensional (3D) information. Here, the existence of information on the initial spectrum is not obligatory in general, especially if the lower detector also measures energy.

Method (b), maybe, merits the right to be called tomography.

Method (a) can become tomography if, after taking several photos (radiographs) from different points, one solves the inverse problem, thus obtaining volumetric information.

3. History and capabilities of the muon radiography method

A proposal to make use of cosmic radiation for resolving problems of geological prospecting (investigation of resources of the lead ore deposits of the Sadon Ore Field) was first voiced by Petr Petrovich Lazarev, founder and first Editor-in-Chief of the journal *Uspekhi Fizicheskikh Nauk* (*UFN*) [26], back in 1926 at a session of the section of physical and mathematical sciences of the General Assembly of the USSR Academy of Sciences (AS). After nearly 30 years, in 1955, P P Lazarev's ideas were partially realized in Australia in measuring the attenuation of a vertical flux of cosmic muons, aimed at assessing the thickness of rocks above a mountainous tunnel [27]. In these studies, a counter telescope was utilized, namely, a detector comprising four rows of Geiger counters. In order to register only the hard component of cosmic radiation, layers of lead 10 cm thick were inserted between the rows of counters. Only particles that passed through all four rows of counters were registered. Thus, any effects related to the background influence of radioactive radiation were excluded. The thickness and mass of rocks was determined by comparing the cosmic ray intensities registered at different sites in the tunnel with the calibration curve. The depth of the tunnel, found with an accuracy of $\pm 5\%$, turned out to be 163.0 ± 8.0 m w.e.

Utilization of the properties of cosmic muons for the purposes of geological prospecting underwent active development in the USSR in the 1960s [28]. In 1961, joint efforts of researchers from the Institute of Terrestrial Magnetism, the Ionosphere, and Radio Wave Propagation USSR AS and a group from the Moscow State Geological Prospecting Institute (MGRI in Russ. abbr.) resulted in the creation of a device for underground registration of cosmic rays, in which two scintillation counters 0.02 m^2 in area were used [29, 30]. The device permitted muon fluxes to be registered in shafts at depths to 100 m with an instrumental error of about 10%. In 1965, in order to enhance the accuracy of underground measurements, a direction-sensitive device, termed the *intensity-meter of cosmic rays*-1 (IMCR-1), was designed and built at the Lebedev Physical Institute of the Russian Academy of Sciences (LPI RAS). It was basically a telescope for mine shafts, consisting of four rows of gas-discharge counters about 1 m^2 in area (12 counters in each row) mounted on a common rotating frame and connected in parallel (Fig. 8).

For studies, a more compact instrument was made using the borehole method, namely, a device for measuring the intensity of cosmic muons with the aid of Cherenkov counters assembled in the form of a small counter telescope about 10 cm in diameter, in which small dimensions were combined

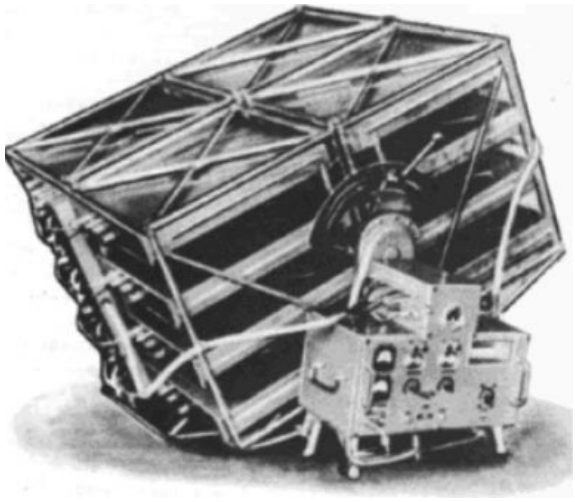

Figure 8. IMCR-1 muon telescope constructed at the Lebedev Physical Institute for performing geological studies in shafts.

with simplicity of assembly and low sensitivity to the radiation from rocks and underground variations of temperature [31]. The device could be lowered into the bore hole, and all the information could be extracted via a cable into the registering equipment on Earth's surface. The measurements of particle fluxes at several underground depths permitted the differential method of determining the densities of individual layers of rock to be applied.

At the end of the 1960s, the muon method was applied for studies of the density of the soil at the site intended for installation of the RATAN-600 radiotelescope of the USSR Academy of Sciences. The gravel soil that served as a natural foundation bed for this construction is, as a rule, very inhomogeneous in composition and actually represents a mixture of boulders, sand, clay, and gravel. Subterranean waters were found at depths of 2 to 8 m from the foundation of the telescope. In these complex hydrogeological conditions alternative methods of determining the soil density are applied very rarely, while the muon method permitted a detailed picture of the soil density distribution to be obtained. The method turned out to be quite noise immune, since the density was determined for large volumes of soil, which excluded the influence of small geological inhomogeneities. Moreover, the choice of such a method was justified by the possibility of using hermetized instruments in shafts filled with water. A total of 35 bore holes were made, in each one of which a small-sized device, the IMCR-2, registering Vavilov–Cherenkov radiation from penetrating muons, was introduced at depths of 3 to 10 m. Data processing made it possible to reconstruct the complex pattern of curves of equal soil density (an isodens map) in the case of density variations from 1.85 to 2.7 g cm^{-3} [31, 32].

In studies carried out at MGRI under the leadership of V M Bondarenko [15], it was shown that a change in the mass of the material above the registering equipment amounting to $\geqslant 10\%$, for example, due to an ore deposit, leads to a change in the muon flux density by a value that can be quite reliably measured during an acceptable (from a practical point of view) period of time. Investigation of the angular distribution of muon fluxes permitted the authors of the design to propose a spatial–angular modification of the muon method, based on simultaneous measurement of the muon fluxes in small solid angles distributed over different zenith and azimuthal directions. The proposed modification permitted improving the resolution over that in the case of integral modification within wide aperture angles.

By the value of the registered muon flux, it is also possible to monitor the laying of mountain tunnels. Determining the fluxes of muons arriving from different directions and, subsequently, the respective distances from Earth's surface (by the general thickness of mountain rock within the field of view of the telescope) at different sites in the tunnel permits checking whether the position of the tunnel inside the mountain corresponds to the design contemplated. A similar method was adopted in estimating the efficiency of radiation shielding of the annular building of the Serpukhov cyclotron of the Institute for High Energy Physics (IHEP), Protvino. The group from MGRI set up the telescope at various points in the annular tunnel of the accelerator and carried out monitoring of the shielding ring ≈ 1.5 km long. As a result, areas were revealed within which, owing to structural features of the construction, as well as other reasons, the protective layer had a mass lower than the required standard [33]. Another example of the application of the MR method in engineering geology is related to the question of determining the pressure exerted by a building on the ground. By putting a detector in a tunnel under the building, one can estimate — by registering the value of the muon flux traversing it — the effective density of the building and determine its mass. The mass of the Moskva Hotel was determined to be about 45 thousand tonnes precisely in this way.

In the 1970s, the muon method based on electronic telescopic equipment was successfully applied in the USSR for solving the following problems:

— determining the properties of naturally deposited rocks, such as the average and layer densities and the loosening coefficient of rock [34, 35];

— detection, positioning and the assessment of orebody capacities at different mines [36, 37];

— revealing and determining breakdown zones in space and time, as well as dealing with tasks related to investigating the efficiency of the biological protection of irradiating equipment [33];

— investigating the accumulation rate of snow in mountain regions with avalanche hazards [38], estimating the pressure exerted by land-based constructions on the ground, etc.

One of the first known foreign experiments, in which the hard cosmic radiation component was utilized, was an investigation of the Egyptian pyramid of Chephren, Giza, performed by a group of scientists led by L W Alvarez [39, 40]. The purpose of this experiment was to search for secret chambers inside the pyramid body, but owing to the insufficient angular resolution of the detector (a spark chamber) and complicated external political circumstances, no quantitative results were obtained. Nevertheless, the method of 'transmitting' pyramids with cosmic rays was considered promising, since it permitted obtaining an image of the pyramid itself in the flux of muons, so it underwent further development. In a similar experiment (Scan Pyramids Project), carried out by an international group of researchers in April 2016, the first 'muonographic' photograph was made of the internal structure of the so-called Bent Pyramid Sneferu at Dahshur, the oldest nonstepped pyramid of Ancient Egypt [41]. The 3D image, obtained with the aid of several emulsion track chambers, permitted previously unknown passages and

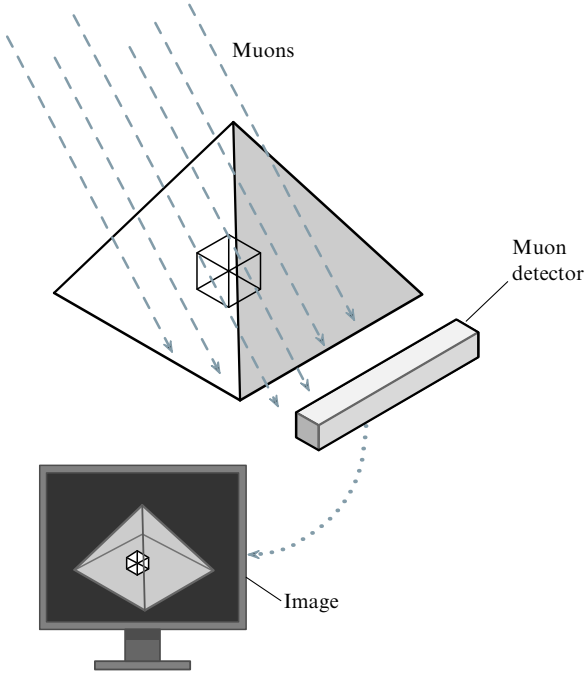

Figure 9. Layout of experiment searching for hidden chambers in the body of a pyramid.

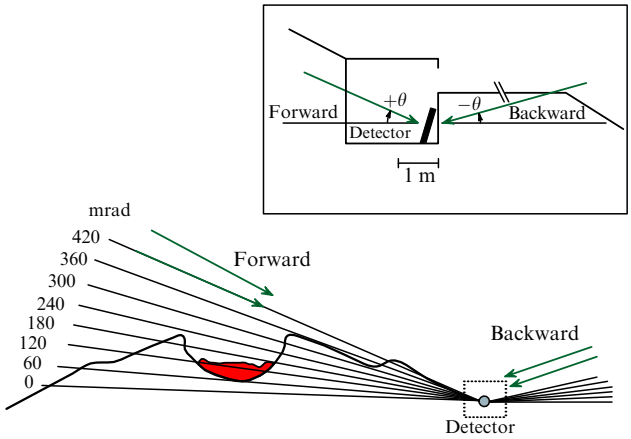

Figure 10. Geometry of an experiment on the investigation of the internal structure of a volcano. The lines show the muon trajectories of the near-horizontal flux registered by the detector [56].

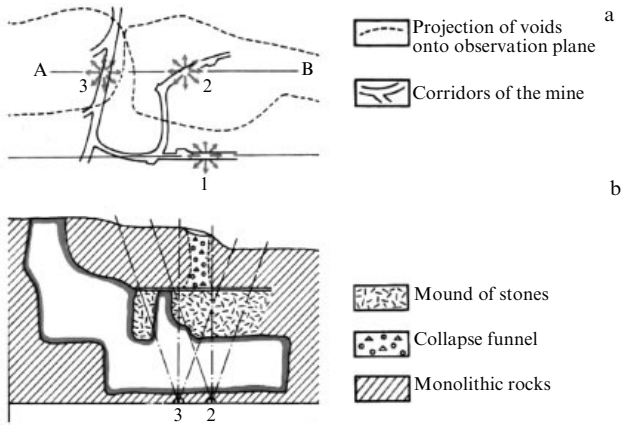

Figure 11. (Color online.) Layout of hodoscopes 1–3 at a depth 250 m in the Tyrnyauz mountain minefield (a) and vertical cross-cut of this deposit along line AB (b). The bold pink curve indicates the contours of the chamber that formed as a result of the extraction of ore in 1973. Two years later, with the aid of a muon detector, the discovery was made that part of the rock forming the ceiling of the chamber broke down, in some points down to the land surface, thus forming a so-called collapse funnel. The dashed–dotted lines in panel (b) show the fields of view of the instruments at points 2 and 3 [59].

chambers to be revealed within the pyramid (Fig. 9). The same group of researchers undertook a search for unknown cavities in the body of the Great Pyramid of Khufu (Cheops). Exposure of the emulsion track detectors during 67 days in the summer of 2016 confirmed with a high confidence level (5σ) the assumption of the existence of a previously unknown cavity behind the northern side of the pyramid [42]. Experiments making use of 'transmission' of archaeological sites continue to be planned [43].[3]

At present, the investigation of volcanoes [45–55] is one of the most common applications of the MP method. These studies are complicated by the existence of uncertainties related to soil composition and the length of muon trajectories, as well as the inhomogeneities of the lava (see Section 4). The problem is resolved by consecutive approximations involving series of angular measurements of the muon flux traversing the mountain, also performed in the background mode (absorption in the atmosphere) for normalization of the angular spectrum to the absolute intensity (Fig. 10).

The important geological problems that the muon radiography method may help to resolve include the investigation of voids in mountain rock. Such voids are often of karst origin, i.e., are formed as a result of soluble compounds (for instance, limestone) being washed out, but they can also be the result of old mines caving in at sites of ore deposits still being exploited [57, 58]. In the Soviet Union, such studies were carried out in 1973–1977 at the Tyrnyauz ore deposit in the North Caucasus (Fig. 11) [59]. Measurements of muon fluxes at one and the same underground point revealed their significant enhancement with time. These time variations of muon fluxes were in good agreement with the assumption that the increase in volume of the empty void was due to the natural collapse of the ceiling and walls of the mine working. Such systematic monitoring of the growth dynamics of voids at deposits being exploited is extremely important for the safety of underground work, since precisely the catastrophic expansion of voids, involving the subsequent rapid break down of rock, creates a serious danger for the extraction of ore from the open pit mining situated above the voids. The MR method permits zones that are dangerous for geological mining to be identified. Voids exhibiting significant density contrasts are favorable subjects for studies by the MR method, since the sensitivity of the method permits revealing and localizing voids, the capacity of which amounts to 5–7% of the observation depth [60]. Moreover, the method provides

[3] During preparation of the present article, a paper was published by K Morishima [44], announcing that a discovery was made, for the first time with the aid of nuclear-photoemulsion detectors, in the Great Pyramid of Khufu (Cheops) of a previously unknown empty chamber 30 m long and with a cross section similar to that of the Grand Gallery. This result was confirmed with a high reliability by two independent measurements by the MP method with the employment of other types of detectors (scintillation and gas detectors). This chamber is the first significant internal structure found in the pyramid since the 19th century.

valuable information on the loosening of broken geological rocks.

At present, development is under way in different countries of new projects for applying the MR method to investigate glacial plates [61], Martian geological sites [62], fire-hazardous coal dumps, industrial sites [63, 64], and facilities in the nuclear power engineering [65], and also to create new methods for geological prospecting of mineral resources [66]. Projects related to monitoring by the MR method the state of the reactor core at the Fukushima-1 nuclear power plant in Japan, damaged by a tsunami in 2011, must be mentioned separately [67].

Most of the studies mentioned are based on the measurements of the flux attenuation of cosmic muons traversing the objects being investigated (so-called one-sided muon radiography based on the absorption method).

An essentially different approach to such studies, known as the method of muon tomography [a method of double-sided radiography (the scattering method) that permits the reconstruction of the in-layer structure of an object by transmitting it repeatedly in intersecting directions], was first proposed in 2003 by researchers at the Los Alamos National Laboratory for controling the unauthorized transportation of nuclear-active materials [68]. The purpose of such experiments is to obtain tomographic images of objects consisting of materials with a large nuclear charge Z, taking advantage of the effect of multiple Coulomb scattering of cosmic muons [69–72]. The equipment comprises two position-sensitive detectors, between which the object of interest is placed. Coordinate detectors provide the track measurements of muons before and after they pass through the volume controlled. The lower detector, within which scattering in a substance of known density takes place, serves for determining the energy of the muons.

Owing to the high energy and to the large mass of the muon, the relatively small deflection of individual muon trajectories (on the order of several milliradians) can be best determined by placing the measuring device immediately before and after the object. Statistical analysis of a certain number of the tracks of muons passing through the volume monitored allows identifying areas inside it exhibiting anomalous scattering of the muons traversing them. The method permits not only separating substances with low and high charges Z and their assignment to nuclear groups (group 1 — C, Al, SiO_2; group 2 — Fe, Ni, Cu, and group 3 — Pb, W, U), but also retrieving the spatial distribution of substances with differing Z [16, 73–79]. It is important that in the case of such an approach — in the double-sided method — the size of the detector must exceed or be comparable to that of the object, whereas in the case of the one-sided method, the object may be significantly larger than the detector, although the detector can also be big. The double-sided method is technically much more complicated, but if it is possible to apply it, then for 'its own' tasks it turns out to be significantly more effective. Performing an experiment with a single detector requires a significantly longer exposure (several months instead of several days); since the use of a single detector in one-sided muon radiography is convenient, it is preferable in those cases when both versions are applicable, and it is rendered indispensable when the size of the object studied is much larger than the size of the detector.

The far from complete list of experiments presented in this section is given to illustrate the range of possibilities provided by the MR method.

4. Equipment for measurements and specific features of experimentation

The measuring equipment for MR comprises drift chambers [80], multiwire proportional chambers (MWPCs) [81, 82], resistive plate chambers (RPCs) [69], etc. In experiments involving the method of one-sided muon radiography, the most utilized electronic equipment based on scintillators is widely applied by Japanese, Italian, and French researchers in studies of the state of volcanoes and tectonic seismic zones [52, 53, 83, 84], as well as the state of blast furnaces [48]. American and Canadian research teams are developing the MR method based on electronic equipment mainly with the aim of searching for mineral resources [66] and monitoring the state of nuclear reactors [65]. As a rule, the registering electronic equipment for one-sided radiography represents hodoscopic devices (telescopes) of a large area, with the aid of which it is possible to detect and identify particles of a certain kind, to establish the angular distribution of radiation, and to determine its absolute intensity [75, 85–88]. The relationship found among the energy of a particle, its energy losses, and the atomic charge of the nucleus can be used when electronic equipment is applied, for instance, for determining the mass of the valuable component of ore bodies, namely, from data on the intensities of individual energy intervals of muons it is possible to estimate deposits of valuable minerals.

An example of the utilization of electronic equipment is the Diaphane experiment — the first European experiment dedicated to investigating volcanoes by the MR method [52, 84, 89]. The detector (telescope), consisting of plastic scintillators, pixel photomultipliers, and an electronic read-out system based on optical fibers, has three independent registering xy-panels with an automatic triggering system (Fig. 12). An event (the transmission of a muon) is registered in a quasi-online mode by sorting out all input signals by their coincidence time. Power is supplied to the detector by solar batteries. Detector power consumption based on plastic scintillators is low, and such detectors are relatively insensitive to the conditions of the environment, which is important in field conditions.

Of all the detectors applied in one-sided MR, the best angular resolution — several milliradians — is exhibited by emulsion track detectors [49, 56, 90–96]. At present, the registration of muons in most experiments takes place in nuclear photoemulsion, deposited on both sides of a triacetate base of dimensions 10×12 cm^2 [97, 98]. Photographic emulsion is a suspension including light-sensitive microcrystals of silver halogenide distributed uniformly in gelatin or another protective colloid [99, 100]. When a charged particle passes through a crystal, energy is absorbed in some of the grains of the emulsion by a crystal of bromide silver, resulting in the formation of an aggregate of a certain number of silver atoms, which can become the center of a hidden image. The formation of a hidden image (i.e., of a track of the ionizing particle that can be developed) in nuclear emulsion is due to the interaction of the charged particle with the electrons of atoms in the emulsion. Thus, owing to its ionizing power, each charged particle penetrating a layer of emulsion leaves a more or less thick track of exposed grains of silver halogenide. After processing the film with a special developer, these grains transform into metallic silver particles and become black, since they consist of finely divided crystalline aggregates. The chemical processing results in the track being visible under a microscope as a chain of separate

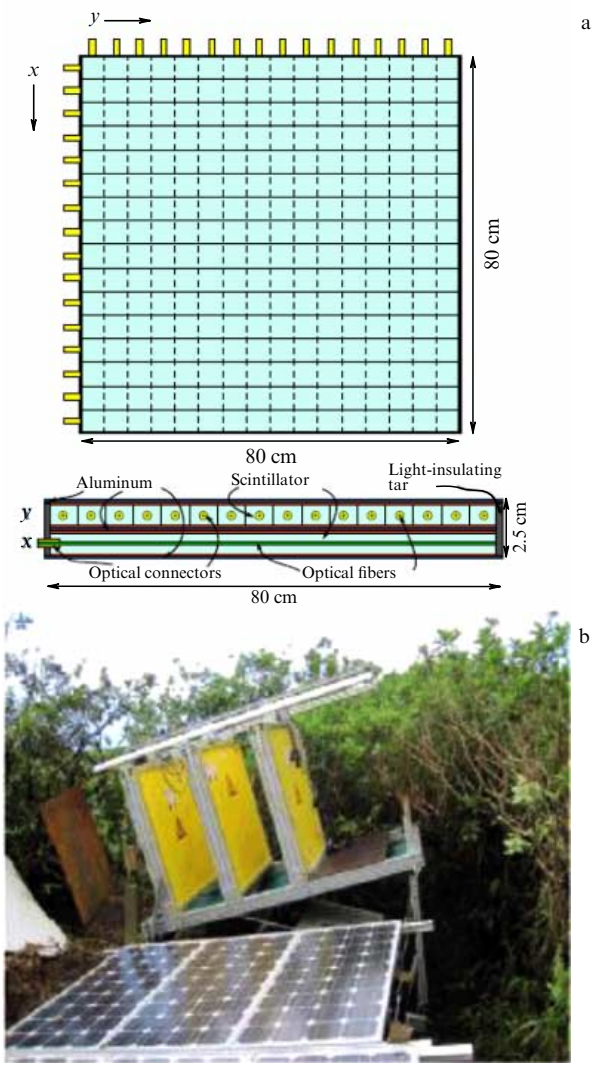

Figure 12. (a) One xy-panel — matrix of 16×16 pixels $0.8 \times 0.8 = 0.64\,\mathrm{m}^2$ in area; the cross section of the panel is shown in the lower part of the figure. (b) Telescopic installation consisting of three registering xy-panels, installed at the site of the experiment [84].

dots or as a solid line, depending on the particle charge (Fig. 13). The chains of developed silver grains permit reconstruction of the particle trajectory in space with a significant precision (the angular measurement accuracy amounts to several milliradians).

Emulsion detectors for MR are autonomous, modular, easy-to-move devices [98] that do not require an additional electricity supply or the presence of an operator, which permits them to compete successfully with electronic detectors for registering probing radiation. About the main advantages of emulsion detectors over electronic equipment, the following can be mentioned.

(1) *High resolution*. This is one of the most important characteristics of emulsion track detectors, caused by the properties of nuclear emulsion. None of the presently known detectors of elementary particles can provide the spatial resolution that is exhibited by nuclear emulsion: given a grain size of 0.3–1 μm, the deviation of grains from the reconstructed trajectory of the particle motion on average does not exceed 0.8 μm, and under certain conditions may equal 0.2 μm. (For comparison, the spatial resolution of a spark chamber is 0.3 mm.) We stress that the use of double-sided emulsion permits achieving a precision in determining angles on the order of several milliradians.

(2) *Possibility of long-term exposure in complicated conditions*. MR emulsion detectors, which are reliably protected from adverse external effects, can be exposed in complex, up to extreme, conditions (for example, close to volcanoes or in conditions of elevated radiation in the zone of damaged nuclear reactors).

(3) *Simple construction and small size of detector*. This permits its installation in the immediate vicinity of the object and is also an advantage for creating a three-dimensional density map of the structure investigated (of an industrial or geological object), when information is obtained from several detectors registering muon fluxes from different points of observation.

(4) *Small size and relative low cost of emulsion detectors*. Their small size, compared, for instance, to that of electronic detectors, which permits achieving the required measurement accuracy, is still another advantage of emulsion detectors (Fig. 14). Track detectors based on nuclear photoemulsions exhibit a significant information capacity, given their relatively small size. Since the amount of emulsion gel required to create a single MR detector varies from several dozen to several hundred grams, the cost of such a detector is quite low.

(5) *Independence of energy supplies*. Emulsion films, which are the basis of MR detectors, do not require any energy

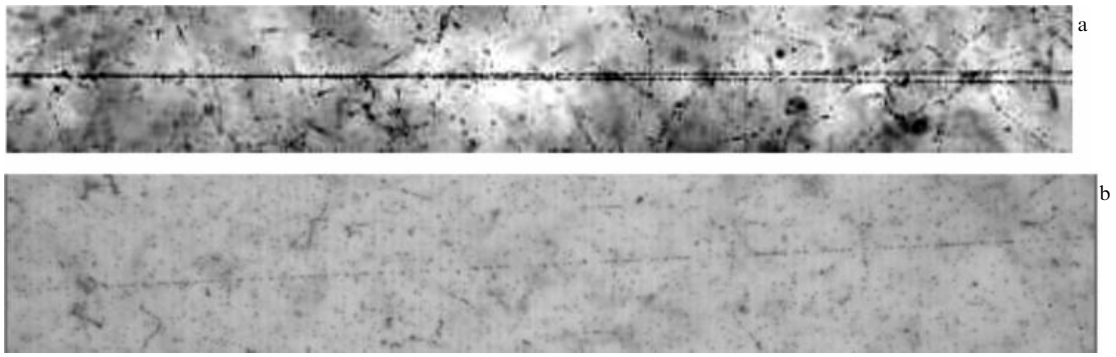

Figure 13. (a) Fragmentation of a relativistic ^{9}Be nucleus and production of two α-particles in nuclear emulsion [101]. The three-dimensional image of the event is reconstructed with the aid of microphotography using the PAVIKOM facility (Russian acronym of *totally automized measuring complex*) (LPI-FIAN) [102]. (b) Track of π-meson with an energy of 10 GeV [102].

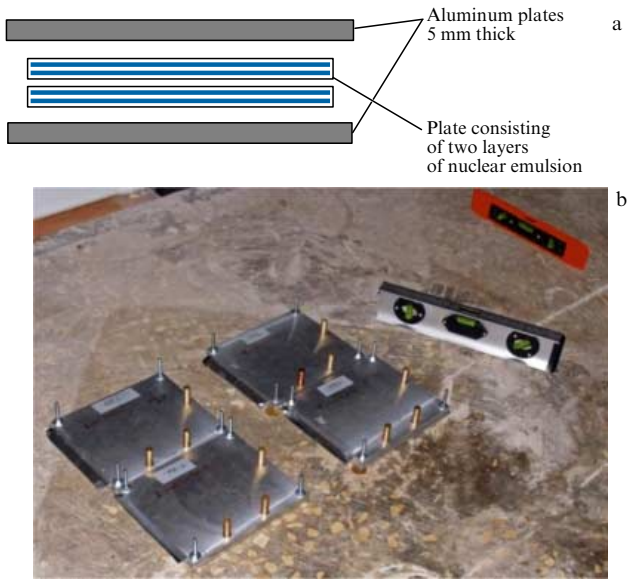

Figure 14. (a) Schematic of a detector assembly with nuclear emulsion 10×12 cm^2 in area fixed with the aid of aluminum plates. (b) Installation of emulsion detectors in an experiment involving MR [98].

supply or electronic read-out system, which is an essential advantage in the complex conditions of experiment.

(6) *Absence of necessity of operative monitoring of the experiment* during the entire exposure time.

Moreover, the detectors themselves are not sources of pollution of the environment.

Regarding the disadvantages of emulsion track detectors, one can mention the impossibility of obtaining data online, the necessity of long-term exposures lasting up to several months, and the difficulty in processing the obtained information. However, owing to the fact that the equipment for automatized measurement is continuously undergoing improvement, the latter disadvantage has been totally overcome. This equipment permits scanning emulsion films with a rate up to 800 cm^2 h^{-1} and a 50× magnification, which, taking into account the micrometer dimensions of tracks, makes possible high-speed processing of large data arrays [67, 103–106]. Emulsion detectors are indispensable in studies of the internal state of nuclear facilities if they have been damaged as a result of a natural disaster or when measurements cannot be performed in any other way (when the facility has been left without any power supply or a danger exists to people remaining in the reactor zone). Thus, precisely emulsion detectors were utilized to control the state of the reactor core at the Fukushima-1 nuclear power plant (Japan) damaged by a tsunami in 2011 [67] (Fig. 15).

Real experiments, in which the method of one-sided muon radiography is applied, exhibit a number of specific features, which, to a greater or lesser, extent complicate interpretation of the obtained data in reconstructing the structure of the object.

(1) The spectrum of cosmic muons is not monochromatic, while the degree of radiation absorption depends on the particle energy, which introduces an uncertainty into the estimation of density for different parts of the object.

(2) The muon flux is subject to variations in time and space that depend on the cycles of solar activity (seasonal, eleven-year cycles related to solar bursts, and others) [10, 107–109]. Additional uncertainties are due to the dependence of the muon flux on the geographic position of the object and are related to Earth's geomagnetic field at a given site, the height of the object above sea level, and weather effects [10, 110]. These uncertainties affect processes with particles of energies $E_\mu \sim 1-10$ GeV. Variations in the fluxes of cosmic particles, the origins of which are quite diverse, may amount to several dozen and even hundreds of percent in Earth's atmosphere; below Earth's surface, however, they do not exceed the limits of 1–3% [111]. The drastic decrease in the amplitude of variations underground is explained by intensity fluctuations in time being mainly related to particles of low energy, which are absorbed at depths inferior to several meters below the land surface. Thus, for example, the amplitude of intensity variations of the muon component underground and on Earth's surface (in periods of absence of solar bursts) does not exceed 3–5%. Consequently, if the muon flux is measured with an uncertainty greater than 3%, the influence of these variations on the registered muon flux can be disregarded. If the measurement accuracy is higher, this sort of noise must be taken into account.

(3) The density of the main part of the irradiated object is, generally, not uniform either, which to a certain extent reduces the difference between the muon fluxes from the main part and from the inhomogeneities investigated. The influence of uncertainty in the chemical composition on the estimation of the density of rocks, which happen to be in the field of view of the detector, is relatively small, especially at small (inferior to 500 m) depths, where muon absorption is only determined by energy losses due to the ionization of atoms of the material. For the effective atomic number and atomic weight of standard mountain rock, the correction for the difference between the chemical composition of standard mountain rock and most types of real rocks does not usually exceed 1–2% [34]. The effect of this factor increases at depths greater than 1 km, where muons of energies $\gtrsim 10^{12}$ eV penetrate to. At such energies, the main effect starts to be caused by other interaction mechanisms (bremsstrahlung, pair production) in which the muon energy losses are proportional to Z^2, i.e., depend more strongly on the chemical composition of the material.

(4) Since in the case of real objects the boundaries between volumes with different densities may be fuzzy, while the actual densities may differ insignificantly, the problem of reconstructing features of the internal structure may require additional calculations.

(5) When experiments are carried out in mountainous terrain, an uncertainty arises that is related to the relief of Earth's surface being complex, when relative elevation or lowering of the relief leads to a respective enhancement of or reduction in the general thickness of material and, respectively, to a change in the underground muon flux. These changes are commensurate in value with flux changes caused, for example, by ore bodies. For this reason, in this case, quite an accurate map of the terrain relief (Digital Elevation Model — DEM) photographed with a sufficient precision is required. There are models with steps 10, 5, and even 1 m, utilized in all work with volcanoes.

The difference in absorption of muons by neighboring parts of the object of interest is due to two reasons: the difference in the muon range within the thickness of the object (i.e., its shape), and the difference in the density of the material. The resulting registered flux is formed under the

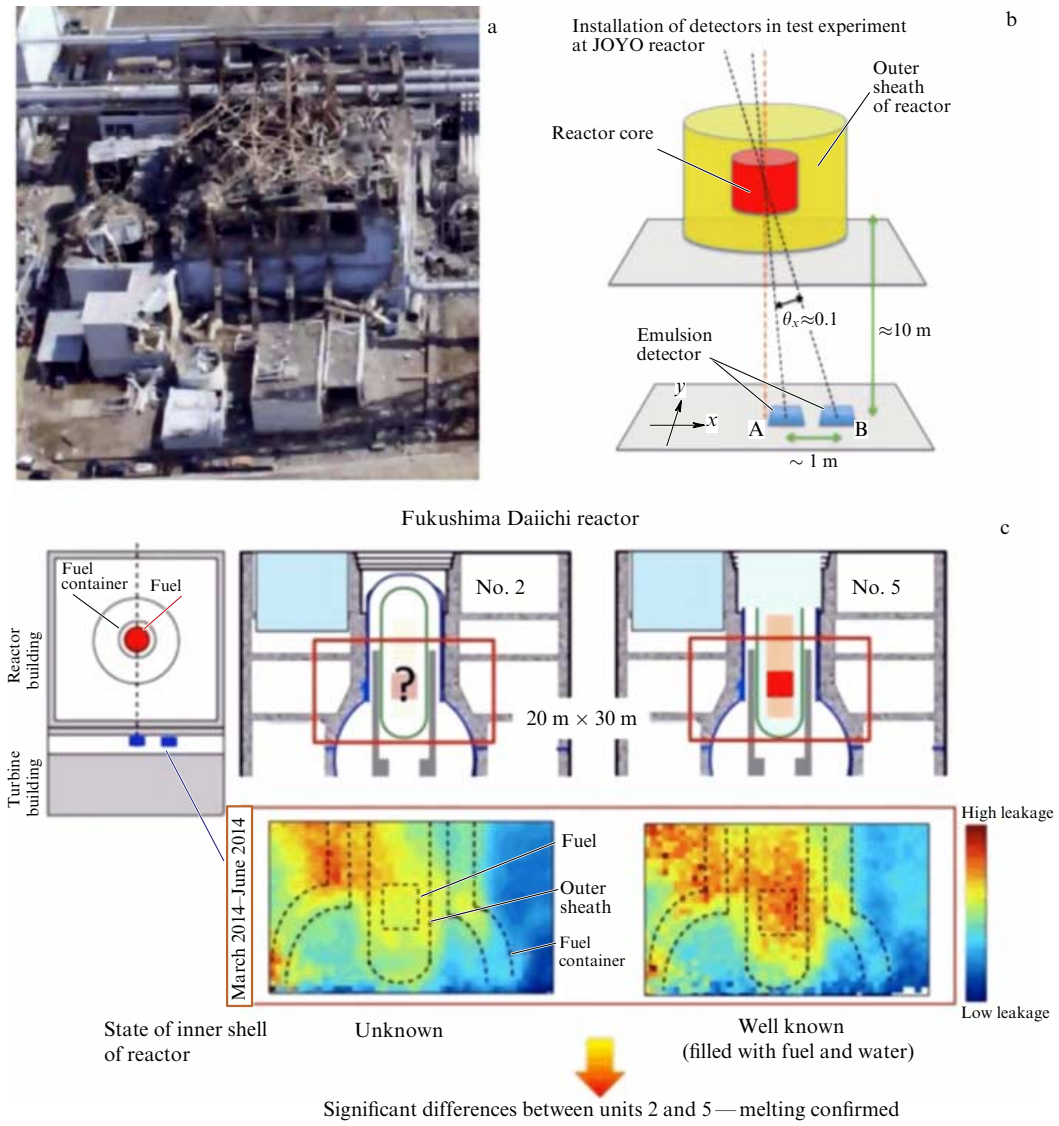

Figure 15. (a) Damaged reactor of the Fukushima nuclear power plant. (b) Layout of emulsion detectors installed at the working JOYO reactor for test experiments aimed at monitoring the state of the reactor by the method of muon radiography; θ_x is the angle in the xy plane. (c) Result of measurements at the damaged Fukushima reactor, obtained with the aid of nuclear-emulsion detectors. Images are presented of two identical nuclear power units, 2 and 5, obtained with the aid of identical emulsion detectors, installed in the same way between March and July 2014. Unit 5 is not damaged, and its reactor is filled with water and fuel. Comparing the images permits us to make conclusions concerning the leakage of material from power unit 2: more than 70% of the fuel melted.

influence of both factors. Since the task of the MR method consists in revealing density inhomogeneities, the effect due to the difference in path lengths in this case is of no interest. To weaken its influence, the authors of this article proposed to use so-called reduced flux values, for example, the ratio of measured fluxes to the path length covered by a muon within the object. Such an approach results in a multiple increase in the efficiency of identifying density inhomogeneities [112]. For planning experiments based on this approach, it is necessary to construct a three-dimensional model of the object of interest, as well as to precisely determine the positions of the detectors with respect to it.

To illustrate this method, the authors of the present article carried out a computer simulation of experimental 'transmission' of a mountain by cosmic muons [113]. The simulation was performed in order to estimate the conditions under which the revelation and investigation of an extended object within the mountain are possible, which has relatively small dimensions and a density differing from the density of the main material. The flux of muons that reach the detector and the direction of their arrival, given by the angular part of spherical coordinates (θ, φ) with their origin at the position of the detector and a vertically directed z-axis (Fig. 16), were chosen as the measured quantities. A hypothetical mountain was chosen as the object, and its three-dimensional model was given by level lines. The detector was installed at a certain distance from it, and 80 rays (16 angles φ and 5 angles θ) were given, which were considered to be muon trajectories — they were used to calculate the numbers of muons that reach the detector. The result of numerical 'measurements' is the projection of the muon flux that reached the detector onto a sphere with its center at the point occupied by the detector. Rocky soil with a density of 2.65 g cm^{-3} was chosen as the material of the mountain. An iron sphere (7.84 g cm^{-3} in density) was placed inside the mountain. Preliminary estimates were

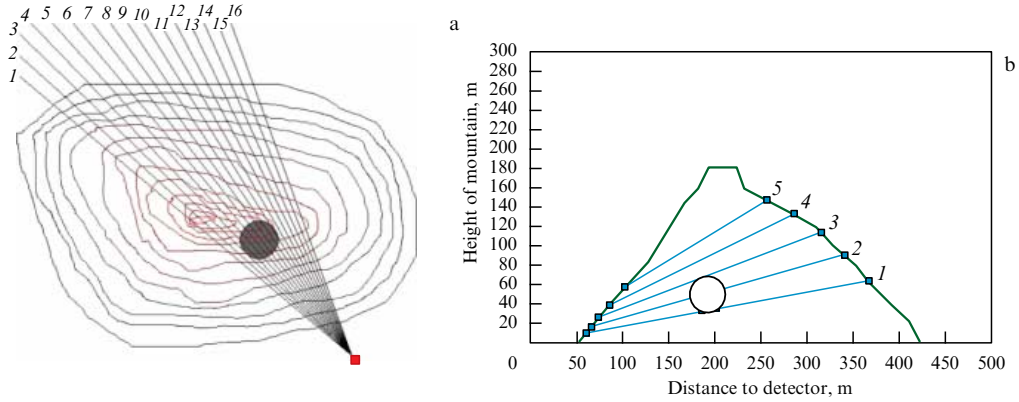

Figure 16. (a) Horizontal projection of the mountain (in the form of level lines), the sphere inside it, the detector (the square in the lower right angle of the figure), and trajectories of muons penetrating the mountain and entering the detector. The numbers *1–16* of the angles φ of trajectories are indicated. (b) Profile of the mountain in the vertical plane crossing trajectory *4* in figure (a). The circle is the cross section of the sphere. Numbers *1–5* indicate angles θ. The detector is situated at the origin of coordinates.

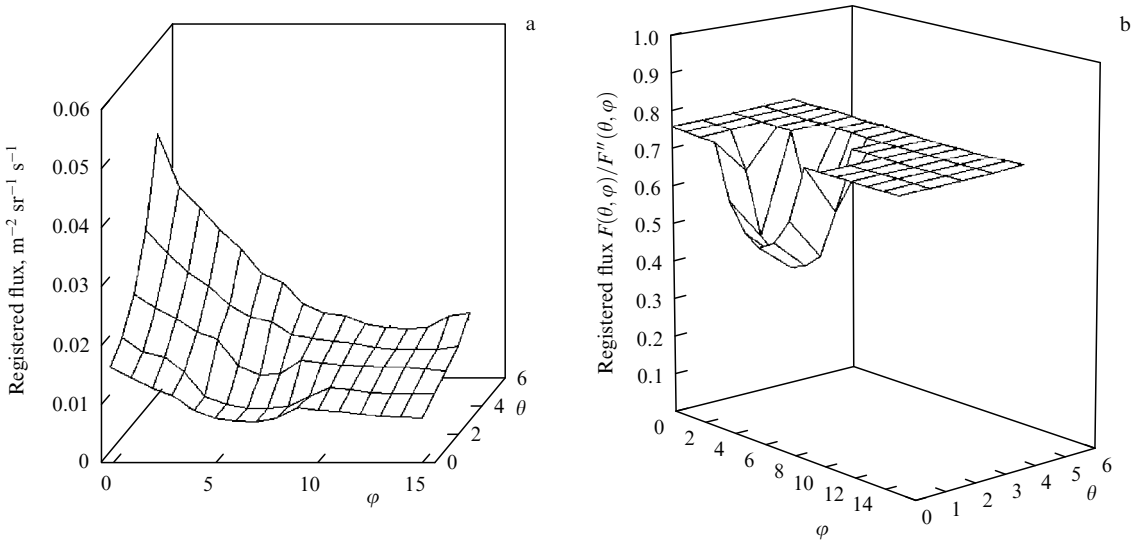

Figure 17. (a) Residual muon flux $F(\theta,\varphi)$ [m^{-2} sr^{-1} s^{-1}] registered at the detector site as a function of the angles in the case of an iron sphere. (b) The reduced flux $F(\theta,\varphi)/F''(\theta,\varphi)$, registered at the detector location as a function of the angles in the case of an iron sphere. As the average density, the density was taken of a material ($\rho = 2.3$ g cm^{-3}) that is not identical to the density of the actual mountain material ($\rho = 2.65$ g cm^{-3}). The values along the φ- and θ-axes correspond to the angle numbers in Fig. 16.

made on the basis of a simplified procedure [23] that took into consideration the shape of the cosmic muon spectrum and the dependence of energy losses on the energy and sort of material, but did not take into account the effect of particle rescattering in the medium, which leads to a change in the direction of the particle trajectories owing to multiple Coulomb scattering and introduces additional uncertainties into the analysis of simulation results [113].

Figure 17a plots the distribution of the flux $F(\theta,\varphi)$ of muons that reached the detector as a function of the angles. The shape of the distribution is seen to be quite smooth, with some irregularities that are difficult to identify as regions of elevated density. For more explicit identification of an alien object in the mountain range, calculations were performed using the flux values presented. To this end, in each of the 80 directions computations were made of the muon path length within the mountain volume and of the muon flux $F''(\theta,\varphi)$ at the output taking into account its attenuation, assuming the uniformity of the material. To show the influence of the true material not coinciding with the material taken to calculate the flux $F''(\theta,\varphi)$, ordinary soil (density of 2.3 g cm^{-3}) was taken in this case. The result of calculations — the ratio F/F'' — is shown in Fig. 17b. The area with density differing from the density of the main material is identified much better. The main material of the mountain may also contain inhomogeneities. If so, in the $\theta-\varphi$ segments of the distribution function, where no alien body is present, inhomogeneities (protrusions and depressions) will also be seen, revealing inhomogeneities of the mountain material itself. Moreover, deviation of the level at which the plane in Fig. 17b is situated from unity characterizes the deviation of the density, taken for calculating F'', from the true density of the main material.

Computations show that experiments with two or more detectors [113] measuring the distribution of an attenuated muon flow through a dense structure from several observation sites are more informative, since in this case it is possible to obtain a 3D distribution of the material in space.

5. Engineering developments in Russia for applying the method of muon radiography based on emulsion track detectors

Until recently, investigations by the MR method in Russia were carried out exclusively with the aid of electronic measuring equipment [114, 115]. No MR experiments making use of emulsion track techniques have been performed in Russia to date because of the absence of a reliable producer of nuclear emulsions with the required quality. However, the creation of the necessary infrastructure for the production of nuclear emulsions at the Russian audio–video company (AVC) Slavich stimulated the interest of scientific groups at Lebedev LPI-FIAN and the D V Skobeltsyn Institute of Nuclear Physics (SINP MSU) in performing test experiments applying the MR method for the first time in Russia. In the experiments, nuclear emulsions produced by the Slavich company were used together, for comparison, with emulsions made by the Japanese company Fuji Photo Film from the OPERA international experiment (Oscillation Project with Emulsion-tRacking Apparatus) [116–118].

The experiment in an underground shaft located in territory belonging to the RAS Geophysical Service in Obninsk [98, 119, 120] was for the authors of the present article the third test experiment at real industrial sites, in which the MR method was applied utilizing nuclear photoemulsion. This work became the first investigation in Russia at an underground site carried out by the MR technique based on track detectors. The facility of the RAS Geophysical Service is a reinforced concrete structure monolithically connected with bedrock and situated at a depth of 30 m within a layer of marbled limestone. During measurements with the aid of emulsion track detectors, the registration was planned of the difference between atmospheric muon fluxes on Earth's surface and beneath it, for which detectors were installed at both levels of observation. The tasks of the experiment also included estimating the possibility of 'revealing' a cylindrical cavity (elevator shaft) within the soil thickness with the aid of detectors situated in the depths (Fig. 18). Figure 18b shows the range of angles θ of cosmic muon trajectories, within which the 'signal' from the elevator shaft should be observed; thus, for example, at $\theta \sim 25^\circ$ and $\varphi \sim 135^\circ$, muon absorption is most weakened by the presence of the void and, correspondingly, the signal must be maximal.

To perform the experiment, six emulsion chambers (D1–D6) were made with six layers of nuclear photoemulsion in each one. To choose the optimal exposure time, irradiation of the detectors in groups was stopped after two and four months. The methods of processing experimental data are presented in detail in Ref. [98]. Analysis of the obtained data revealed that for collecting the necessary statistics in the case of detector irradiation in underground chambers at a depth of 30 m, an exposure within two months is insufficient. Therefore, the main results were obtained with films irradiated for four months.

An illustrative way of presenting the data consists in examining the dependence of the number of muons registered by the detector on the azimuthal incidence angle φ (the data were summed over the zenith angles within the range of registration $\theta = 0-45^\circ$). In such a representation, the presence of the signal is clearly seen because of the existence of a void in the soil, formed by the vertical elevator shaft.

According to the results of the experiment, the muon fluxes in the land-based and underground (at a depth of 30 m) detectors differ by a factor of about 50 (thus, for the same exposure time, the number of tracks in the land-based detector D1 amounted to 31,136 for every 30 cm^2, and in the underground detector D5 — 671 for every 30 cm^2). The track density distributions of cosmic muons in the emulsion obtained in the experiment were represented in variables $\sin\varphi\sin\theta$ and $\cos\varphi\sin\theta$ determining the inclination of muon trajectories with respect to the normal to the detector plane. Figure 19a plots the experimental two-dimensional distribution of the muon flux obtained after a four-month exposure in one of the detectors 30 m beneath the surface, after subtracting the averaged background. An additional coordinate grid of angles is drawn in the figure: of the azimuthal angle φ (rays departing from the center with a 15° step) and of the zenith angle θ (circles *1*, *2*, and *3* drawn for angles $\theta = 15^\circ$, 30°, and 45°, respectively). In such coordi-

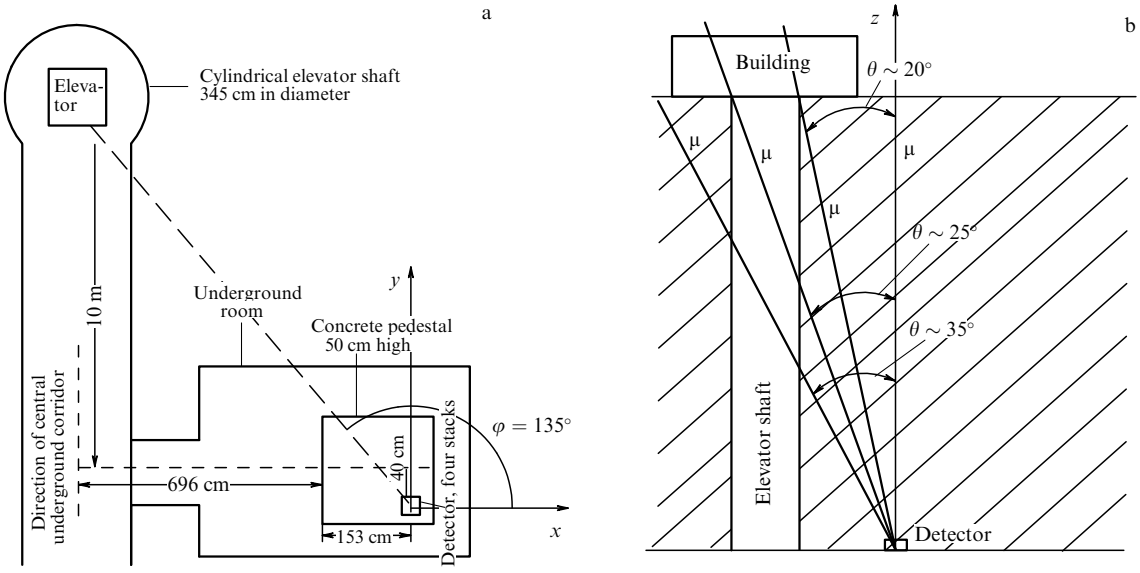

Figure 18. Horizontal (a) and vertical (b) outlines of the FIAN–SINP MSU experiment [119]. The disposition of the coordinate axes is indicated in the detector system.

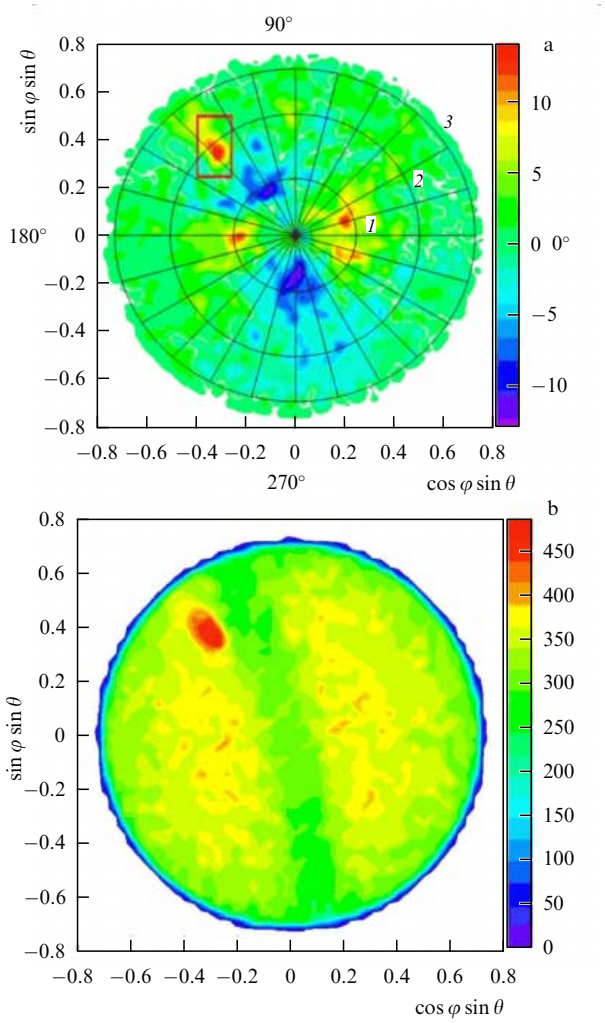

Figure 19. (Color online.) (a) Two-dimensional track density distribution of cosmic muons in a shaft at a depth of 30 m. The rectangle indicates the location of the elevator shaft. The coordinate grid shows the lines of constant angles: rays departing from the center with a step of 15° correspond to angles φ, while circles *1–3* correspond to angles $\theta = 15°$, 30°, and 45°. (b) Calculated distribution obtained from the results of the simulation described in Ref. [120]. A spot is clearly seen that corresponds to a significant increase in the muon flux density due to the presence of a shaft in the ground. The track density distributions are presented in terms of the variables $\sin\varphi\sin\theta$ and $\cos\varphi\sin\theta$, determining the inclination of muon trajectories with respect to the normal to the detector plane. In such coordinates, the distance between a certain point and the center on the scale of the figure equals $\sin\theta$.

nates, the distance from a certain point to the center on the scale of the figure equals $\sin\theta$. The experimental distributions clearly show the elevator shaft and a number of other structural peculiarities of the construction examined. The number of tracks in each bin in the zone of the elevator shaft (indicated by the red frame) varies from 60 to 100, i.e., the data presented are statistically secure. The experiment performed clearly demonstrates the potential of the MR method based on the emulsion track technique.

Simulations of this experiment were also carried out using GEANT4 software package [120]. Simulation was performed of 10 million muons traversing the soil thickness and the zone of the elevator shaft, and a picture of the angular distribution of the muon flux that hit the detector was constructed. The results of numerical simulations showed good agreement with experimental data concerning the problem of finding the cavity of the elevator shaft represented in an analogous manner (Fig. 19b).

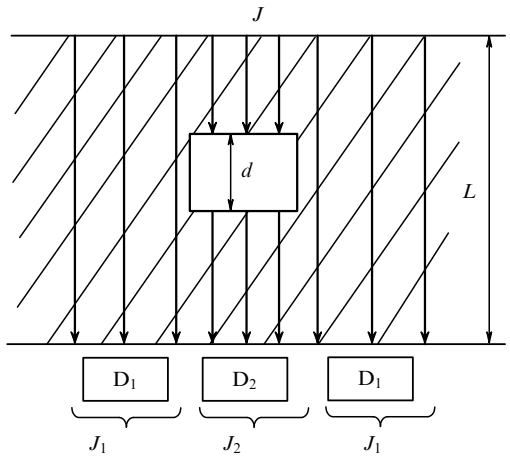

Figure 20. Schematic of experiment to assess the sensitivity of the MR method.

6. Assessment of the method sensitivity

Under the sensitivity of the method is understood its capability of revealing an inhomogeneity of minimal mass and volume, creating such an anomalous change in the muon flux density that can, to a sufficient degree, be reliably registered, given the measurement error. The information value of the method is determined by the error in the muon flux density measurement, the number of zenith–azimuthal directions along which these fluxes are measured simultaneously, and by the depth of observation.

Let us assume a cavity of dimension d (Fig. 20) exists in a layer of ground of thickness L. This layer is irradiated by a flux of cosmic muons, J_0, and registered by the lower row of detectors (D_1, D_2). The fluxes in the detectors registering muon fluxes that do not pass (J_1) and that do pass (J_2) through the cavity differ from each other. If the observable flux is J, we denote by ΔJ the minimum difference between muon fluxes distinguishable by a detector, and by $S = \Delta J/J$ the detector sensitivity. Then, for given values of L and S there is a minimum dimension d of the cavity that can be distinguished by the detector. The corresponding condition is given by $(J_2 - J_1)/J_1 = S$.

In Table 1, relations are presented among L, d, and S for ground of density 2.3 g cm^{-3}, obtained taking into account the degree of absorption of cosmic muons and their spectrum, applying a simplified procedure [23].

In the case of a more detailed consideration, not only is the ray sensitivity of the method, i.e., the minimum dimensions of identified objects in the direction of the cosmic ray flux, dealt with, but so is the transverse sensitivity, i.e., the minimum length and width of the inhomogeneity identified.

Table 1. Sensitivity assessments of the MR method.

Distance L from the surface to the detector, m	Sensitivity S, %			
	5	10	20	30
50	$d = 1$ m	$d = 2$ m	$d = 5$ m	$d = 8$ m
100	$d = 3$ m	$d = 5$ m	$d = 7$ m	$d = 14$ m

7. Conclusion. Muon georadiography

On the basis of the above, one can speak of the resurrection in Russia, at a qualitatively new level, of the MR method — a promising technology for various areas of studies in science and applications. To judge the prospects of the method, it is necessary to assess its advantages, as well as its possible limitations.

As was shown above, the method of probing dense extended objects with the aid of penetrating cosmic radiation is based on simple and rigorous physical fundamentals, established as a result of theoretical and experimental studies in physics, carried out during many decades both in Russia and abroad. The results of these studies have been applied, for example, in resolving certain geophysical problems. The development of the geological aspect of the MR method has demonstrated the possibility of making use of cosmic rays along three main avenues of investigation:

(1) for resolving certain exploratory and ecological problems in ore deposits (investigating regions that are promising from the point of view of the presence of minerals, the revelation of focal fire zones of carbon dumps, etc.);

(2) for resolving issues related to engineering-geological and hydrogeological problems;

(3) for determining the average density value of mountain rock.

Underground gravimetrical prospecting and radio wave transmission are rivals of the MR method in geological prospecting. Gravimetrical prospecting is based on differences in magnitudes of the gravitational effect arising from the distribution of masses [121]. In the case of underground modification of gravimetrical prospecting, an uncertainty appears related to the fact that at points of the underground profile the total gravitational effect is registered from masses lying higher and lower, and the problem arises of distinguishing their contributions. The ways to resolve this problem are based on the assumption that the mass distribution above the observation profile is known, in other words, information exists on the density of mountain rock and inhomogeneities, their thickness, and the distance to the observation point. In a number of cases, these quantities are known with insufficient accuracy, which leads to errors in the interpretation of gravitational prospecting data. The MR method has no such disadvantages.

The method of radio wave transmission, based on differences in the absorption of radio waves by mountain rocks, can be applied to search for ore bodies and to determine their contours [122] and to investigate the state of bridge supports [123]. However, this method cannot provide information on parameters such as the density of mountain rock or the distribution of mountain rock masses. Moreover, the method of radio wave transmission requires an artificial source of electromagnetic radiation, which, naturally, complicates performance of the work and raises its cost. To implement this method, at least two open pit minings or wells are required. In addition, the equipment utilized exhibits relatively low long-range action, especially within low-ohmic rocks, where radio waves are almost completely damped at a distance from 100 to 120 m.

The MR method can reach depths up to 2–3 km, i.e., such depths at which cosmic muon fluxes are registered, although, here, the exposure time required to obtain statistically significant results increases considerably. The existence of a natural source of high-energy penetrating particles of cosmic radiation permits information to be obtained with the aid of a single level of detectors of these particles (one-sided muon radiography). To this end, besides electronic equipment, an economical, simple, and safe technology that does not require additional power supplies and is based on nuclear photoemulsions is at present under development and is successfully competing in this area of research with electronic methods of registering elementary particles.

The advantages of the MR method based on nuclear emulsions, which distinguishes it from the series of alternative probing methods applied at present, are the following:

— high penetration power of the probing radiation (cosmic muons);

— high angular and spatial resolution of the detectors;

— possibility of creating a three-dimensional image of the object;

— artificial radiation sources not required;

— independence from power supplies;

— not necessity to operatively monitor the experiment during the entire exposure.

A consequence is also a significant reduction in the cost of work making use of emulsion MR detectors compared with work involving other methods.

The following must be considered limitations of the MR method. First, the method can provide information only on material lying above the level of the registering equipment (or at an angle to the detector). Thus, for geological prospecting this implies the existence of horizontal excavations or wells as a necessary condition for applying the MR method. The second disadvantage is related to the fact that, to achieve the necessary and sufficient observation accuracy, the time of detector exposure increases drastically at large depths. The indicated particular disadvantages of the method in no way detract from its qualities exhibited in the course of resolving a number of practical problems.

Thus, in this article, the material concerning developments and tests of the MR method based on the registration of penetrating cosmic radiation is systematized. The physical fundamentals and observation technique are presented, and methods and instruments for the registration of penetrating muons are considered. The method has been successfully tested, which is confirmed by the results obtained applying this method by the authors of this article in several of the first on-site experiments. Methods for simulation and processing experimental results are described along with some methods of interpreting the data obtained. Special attention is paid to comparing the results of one of the test experiments, performed by the authors, and information on the geological structure of the work sites. An outline is given of the further development of the MR method. All the foregoing points to the expediency and possibility of developing and applying what is quite new in the world and absolutely new in Russia, namely the MR method with the usage of emulsion track detectors and means of processing emulsion data that are presently at the disposal of Russian institutions.

References

1. Allkofer O C, Grieder P K F *Cosmic Rays on Earth*: *Physics Data* (Karlsruhe: Fachinformationszentrum Energie, Physik, Mathematik GmbH, 1984)
2. Beringer J et al. (Particle Data Group) *Phys. Rev. D* **86** 010001 (2012)

3. Bugaev E V et al. *Phys. Rev. D* **58** 054001 (1998)
4. Groom D E, Mokhov N V, Striganov S I *At. Data Nucl. Data Tabl.* **78** 183 (2001)
5. Barkas W H, Birnbaum W, Smith F M *Phys. Rev.* **101** 778 (1956)
6. Bichsel H *Phys. Rev. A* **41** 3642 (1990)
7. Schultz L J, A Dissertation for the Degree of Doctor of Philosophy in Electrical and Computer Engineering (Portland: Portland State Univ., 2003)
8. Menon M G K et al. *Can. J. Phys.* **46** S344 (1968)
9. Aglietta M et al. (LVD Collab.) *Phys. Atom. Nucl.* **66** 123 (2003); *Yad. Fiz.* **66** 125 (2003)
10. Cecchini S, Spurio M *Geosci. Instrum. Method. Data Syst.* **1** 185 (2012)
11. Grieder P K F *Extensive Air Showers*: *High Energy Phenomena and Astrophysical Aspects — A Tutorial, Reference Manual and Data Book* (Heidelberg: Springer, 2010)
12. Varey G W, A Dissertation for the Degree of Master of Science in Radiation Detection and Instrumentation (Surrey: Univ. of Surrey, 2010)
13. Patrignani C et al. (Particle Data Group) *Chin. Phys. C* **40** 100001 (2016)
14. Costa C G S *Astropart. Phys.* **16** 193 (2001)
15. Bondarenko V M, Doctoral Dissertation (Moscow: Moscow Geological Prospecting Institute, 1982)
16. Schultz L J et al. *Nucl. Instrum. Meth. Phys. Res. A* **519** 687 (2004)
17. Lynch G R, Dahl O I *Nucl. Instrum. Meth. Phys. Res. B* **58** 6 (1991)
18. Nakamura K, Particle Data Group *J. Phys. G* **37** 075021 (2010)
19. Longhin A, Paoloni A, Pupilli F *IEEE Trans. Nucl. Sci.* **62** 2216 (2015)
20. Agostinelli S et al. *Nucl. Instrum. Meth. Phys. Res. A* **506** 250 (2003)
21. Allison J et al. *Nucl. Instrum. Meth. Phys. Res. A* **835** 186 (2016)
22. Clarkson A et al. *Nucl. Instrum. Meth. Phys. Res. A* **746** 64 (2014)
23. Zemskova S G, Starkov N I *Bull. Lebedev Phys. Inst.* **42** 157 (2015); *Kratk. Soobshch. Fiz.* **42** (6) 3 (2015)
24. Herman G T *Fundamentals of Computerized Tomography*: *Image Reconstruction from Projections* (Dordrecht: Springer, 2009)
25. Erlandson A et al. *CNL Nucl. Rev.* (2016); https://doi.org/10.12943/CNR.2016.00014
26. Kravkov S V *Usp. Fiz. Nauk* **46** 441 (1952)
27. George E P *Commonwealth Engineer* 455 (1955)
28. Bondarenko V M *Ispol'zovanie Kosmicheskikh Luchei v Geologii* (Application of Cosmic Rays in Geology) (Moscow: Nedra, 1965)
29. Blokh Ya L, Bondarenko V M, Tarkhov A G *Geomagn. Aeronom.* **2** 390 (1963)
30. Bondarenko V M, Zhdanov G B *Priroda* (8) 20 (1980)
31. Bondarenko V M et al. *Novye Metody Inzhenernoi Geofiziki* (New Methods of Geophysical Engineering) (Moscow: Nedra, 1983)
32. Bondarenko V M, Viktorov G G, Tarkhov A G *Sov. Geolog.* (6) 85 (1970)
33. Bondarenko V M, Viktorov G G, Tarkhov A G *Sov. Atom. Energy* **24** 411 (1968); *At. Energ.* **24** 330 (1968)
34. Viktorov G G, Bondarenko V M *Myuonnyi Metod Opredeleniya Plotnosti Gornykh Porod* (Muon Method for Determining the Density of Mountain Rock) (Moscow: Atomizdat, 1973)
35. Bondarenko V M et al. *Sov. Atom. Energy* **36** 656 (1974); *At. Energ.* **36** 518 (1974)
36. Chertkov V Ya, Tarkhov A G, Bondarenko V M, in *Razvedochnaya Geofizika SSSR na Rubezhe 70-kh Godov* (USSR Geophysical Prospecting at the Boundary of the 1970s) (Ed. V V Fedynskii) (Moscow: Nedra, 1974) p. 389
37. Bondarenko V M, in *Razvedochnaya Geofizika SSSR na Rubezhe 70-kh Godov* (USSR Geophysical Prospecting at the Boundary of the 1970s) (Ed. V V Fedynskii) (Moscow: Nedra, 1974) p. 409
38. Avdyushin S I et al. *Meteorolog. Gidrolog.* (12) 83 (1973)
39. Alvarez L W et al. *Science* **167** 832 (1970)
40. Wohl C G *Am. J. Phys.* **75** 968 (2007)
41. Press Release of Heritage Innovation Preservation. HIP Institute, Cairo, the 17th of December 2015: Muons Detectors plates installed at Bent Pyramid and under sensitivity calibration in Khufu's Pyramid, http://www.hip.institute/press/HIP_INSTITUTE_CP5_EN.pdf
42. Press Release of Heritage Innovation Preservation. HIP Institute, Cairo, October 15th, 2016: #ScanPyramids. First conclusive findings with muography on Khufu Pyramid, http://www.hip.institute/press/HIP_INSTITUTE_CP9_EN.pdf
43. Gómez H et al. *J. Phys. Conf. Ser.* **718** 052016 (2016)
44. Morishima K *Nature* (2017) publ. online November 2017; https://doi.org/10.1038/nature24647
45. Nagamine K et al. *Nucl. Instrum. Meth. Phys. Res. A* **356** 585 (1995)
46. Nagamine K *J. Geography* **104** 998 (1995)
47. Tanaka H et al. *Nucl. Instrum. Meth. Phys. Res. A* **507** 657 (2003)
48. Nagamine K et al. *Proc. Jpn. Acad. B* **81** 257 (2005)
49. Tanaka H K M et al. *Am. J. Sci.* **308** 843 (2008)
50. Tanaka H K M et al. *J. Geophys. Res.* **115** B12332 (2010)
51. Buontempo S et al. *Earth Planets Space* **62** 131 (2010)
52. Marteau J et al. *Nucl. Instrum. Meth. Phys. Res. A* **695** 23 (2012)
53. Cârloganu C et al. *Geosci. Instrum. Method. Data Syst.* **2** 55 (2013)
54. Ambrosino F et al. *JINST* **9** C02029 (2014)
55. Catalano O et al. *Nucl. Instrum. Meth. Phys. Res. A* **807** 5 (2016)
56. Tanaka H K M et al. *Earth Planet. Sci. Lett.* **263** 104 (2007)
57. Tanaka H K M, Muraoka H *Geosci. Instrum. Method. Data Syst.* **2** 145 (2013)
58. Konovalova N S, Polukhina N G *Innovatika Ekspertiza* (2) 52 (2015)
59. Bondarenko V M et al. "Primenenie metoda podzemnoi registratsii kosmicheskogo izlucheniya dlya resheniya nekotorykh gorno-tekhnicheskikh zadach" ("Application of the method of underground registration of cosmic radiation for performing certain mining and technical tasks"), in *Metody Razvedochnoi Geofiziki* (Methods of Geophysical Prospecting) (Leningrad: NPO Geofizika, 1978) p. 55
60. Bondarenko V M *Kosmicheskie Luchi v Geologii*: *Myuonnyi Metod* (Cosmic Rays in Geology: the Muon Method) (Review Information. Ser. Regional Prospecting and Commercial Geophysics) (Moscow: VIEMS, 1979)
61. Nishiyama R et al. *Geophys. Res. Abstracts* **18** EGU2016-11722 (2016)
62. Kedar S et al. *Geosci. Instrum. Method. Data Syst.* **2** 157 (2013)
63. Tanaka H K M *Geosci. Instrum. Method. Data Syst.* **2** 79 (2013)
64. Jourde K et al. *Sci. Rep.* **6** 23054 (2016)
65. Durham J M et al. *AIP Adv.* **5** 067111 (2015)
66. Bryman D, Bueno J, Jansen J *ASEG Exten. Abst.* (1) 1 (2015)
67. Fukuda T et al. *JINST* **8** P01023 (2013)
68. Borozdin K N et al. *Nature* **422** 277 (2003)
69. Morris C L et al. *Sci. Global Security* **16** 37 (2008)
70. Syresin D E, Shelkov G A *Phys. Part. Nucl. Lett.* (6) 465 (2009); *Pis'ma Fiz. Elem. Chastits At. Yadra* (6) 769 (2009)
71. Baesso P et al. *JINST* **9** C10041 (2014)
72. Morris C L et al. *Nucl. Instrum. Meth. Phys. Res. B* **330** 42 (2014)
73. Jonkmans G et al. *Ann. Nucl. Energy* **53** 267 (2013)
74. Perry J O et al. *J. Appl. Phys.* **115** 064904 (2014)
75. Clarkson A et al. *Nucl. Instrum. Meth. Phys. Res. A* **745** 138 (2014)
76. Woo J J et al. *J. Korean Phys. Soc.* **66** 585 (2015)
77. Anghel V et al. *Nucl. Instrum. Meth. Phys. Res. A* **798** 12 (2015)
78. Burns J et al. *JINST* **10** P10041 (2015)
79. Åström E et al. *JINST* **11** P07010 (2016)
80. Zadeba E A et al. *Bull. Russ. Acad. Sci. Phys.* **79** 377 (2015); *Izv. Ross. Akad. Nauk Ser. Fiz.* **79** 411 (2015)
81. Oláh L et al. *Adv. High Energy Phys.* **2013** 560192 (2013)
82. Oláh L et al. *J. Phys. Conf. Ser.* **632** 012020 (2015)
83. Tanaka H K M et al. *Earth Planet. Sci. Lett.* **306** 156 (2011)
84. Lesparre N et al. *Geosci. Instrum. Method. Data Syst.* **1** 33 (2012)
85. Yadav C et al. *Proc. DAE Symp. Nucl. Phys.* **56** 1066 (2011)
86. Barnaföldi G G et al. *Nucl. Instrum. Meth. Phys. Res. A* **689** 60 (2012)
87. Oláh L et al. *Geosci. Instrum. Method. Data Syst.* **1** 229 (2012)
88. Bonechi L *JINST* **10** P02003 (2015)
89. Gibert D et al. *Earth Planets Space* **62** 153 (2010)
90. Tanaka H K M et al. *Nucl. Instrum. Meth. Phys. Res. A* **575** 489 (2007)
91. Tanaka H K M et al. *Geophys. Res. Lett.* **34** L22311 (2007)
92. Tanaka H K M, Yokoyama I *Proc. Jpn. Acad. B* **84** 107 (2008)
93. Ariga A et al. *Geophys. Res. Abst.* **13** EGU2011-8977 (2011)
94. Consiglio L, Tioukov V *Astropart. Part. Space Phys. Radiat. Interact. Detect. Med. Phys. Appl.* **8** 708 (2014)
95. Nishio A et al. *Phys. Procedia* **80** 74 (2015)
96. Ariga T et al. *JINST* **11** P03003 (2016)

97. Aleksandrov A B et al. *AIP Conf. Proc.* **1702** 110002 (2016)
98. Baklagin S A et al. *Int. J. Innov. Res. Sci. Eng. Technol.* **5** 0507027 (2016)
99. Powell C F, Fowler P H, Perkins D H *The Study of Elementary Particles by the Photographic Method*: *An Account of the Principal Techniques and Discoveries, Illustrated by an Atlas of Photomicrographs* (London: Pergamon Press, 1959)
100. Morishima K *Phys. Procedia* **80** 19 (2015)
101. Artemenkov D A et al. *Phys. Atom. Nucl.* **70** 1222 (2007); *Yad. Fiz.* **70** 1261 (2007)
102. Aleksandrov A B et al. *Nucl. Instrum. Meth. Phys. Res. A* **535** 542 (2004)
103. Bozza C, Nakano T, in *Current Microscopy Contributions to Advances in Science and Technology* Vol. 2 (Ed. A Méndez-Vilas) (Badajoz: Formatex, 2012) p. 1511
104. Alexandrov A, Tioukov V *Nucl. Instrum. Meth. Phys. Res. A* **718** 184 (2013)
105. Alexandrov A, Tioukov V, Vladymyrov M *JINST* **9** C02034 (2014)
106. Alexandrov A et al. *JINST* **10** P11006 (2015)
107. Belov A et al. *Solar Phys.* **290** 1429 (2015)
108. Balabin Yu V, Belov A V, Gushchina R T *Bull. Russ. Acad. Sci. Phys.* **79** 622 (2015); *Izv. Ross. Akad. Nauk Ser. Fiz.* **79** 676 (2015)
109. Adamson P et al. (MINOS Collab.) *Phys. Rev. D* **91** 112006 (2015)
110. Ampilogov N V et al. *Astrophys. Space Sci. Trans.* **7** 435 (2011)
111. Dorman L I *Cosmic Rays: Variations and Space Explorations* (Amsterdam: North-Holland, 1974); Translated from Russian: *Variatsii Kosmicheskikh Luchei i Issledovanie Kosmosa* (Moscow: Izd. AN SSSR, 1963)
112. Tarkhov A G, Bondarenko V M, Nikitin A A *Kompleksirovanie Geofizicheskikh Metodov* (Complexing of Geophysical Methods) (Moscow: Nedra, 1982)
113. Starkov N I *Bull. Lebedev Phys. Inst.* **41** 76 (2014); *Kratk. Soobshch. Fiz.* **41** (3) 39 (2014)
114. Zemskova S G, Starkov N I *Bull. Lebedev Phys. Inst.* **42** 37 (2015); *Kratk. Soobshch. Fiz.* **42** (2) 11 (2015)
115. Bondarenko V M, Brovkin V I, Tarkhov A G *Izv. Vyssh. Uchebn. Zaved. Geolog. Razvedka* (8) 61 (1973)
116. Borisov A A et al. *Instrum. Exp. Tech.* **55** 151 (2012); *Prib. Tekh. Eksp.* (2) 5 (2012)
117. Nakamura T et al. *Nucl. Instrum. Meth. Phys. Res. A* **556** 80 (2006)
118. Ariga A, OPERA Collab. *AIP Conf. Proc.* **981** 175 (2008)
119. Agafonova N et al. (OPERA Collab.) *Phys. Rev. Lett.* **115** 121802 (2015)
120. Aleksandrov A B et al. *Phys. Part. Nucl. Lett.* **12** 713 (2015); *Pis'ma Fiz. Elem. Chastits At. Yadra* **12** 1100 (2015)
121. Aleksandrov A B et al. *Bull. Russ. Acad. Sci. Phys.* **81** 500 (2017); *Izv. Ross. Akad. Nauk Ser. Fiz.* **81** 538 (2017)
122. Utemov E V *Gravirazvedka*: *Posobie dlya Samostoyatel'nogo Izucheniya Lektsionnogo Kursa Slushatelei Kursov Povysheniya Kvalifikatsii Spetsial'nosti Geofizika* (Manual for Self-Study of a Lecture Course by Listeners of Refresher Courses in Geophysics Specialty) (Kazan: Kazan. Gos. Univ., 2009)
123. Istratov V A *Inzhenern. Izyskaniya* (4) 78 (2008)
124. Panov V S *Inzhenern. Izyskaniya* (10) 54 (2012)